Optimization Geometry of zhe Body Presses for the fine punching using FEM Analyzis

Article · January 2014

CITATIONS
0

READS
95

5 authors, including:

Radomir Radiša
Lola Institut
31 PUBLICATIONS **249** CITATIONS
SEE PROFILE

Srecko Manasijevic
Lola Institute Ltd
47 PUBLICATIONS **290** CITATIONS
SEE PROFILE

Vesna Mandic
Faculty of Science, University of Kragujevac
26 PUBLICATIONS **158** CITATIONS
SEE PROFILE

Velimir Komadinić
Lola Institut
6 PUBLICATIONS **9** CITATIONS
SEE PROFILE

UNIVERSITY OF NOVI SAD
Faculty of Technical Sciences
Department of Production Engineering
NOVI SAD, SERBIA

UDK 621

ISSN 1821-4932

JOURNAL OF
PRODUCTION ENGINEERING

Volume 17

No.2

Novi Sad, 2014

Journal of Production Engineering
Vol.17 No.2

Original Scientific Paper

Radiša, R., Manasijevic, S., Mandic, V., Stefanovic, M., Komadinic, V.

OPTIMIZATION GEOMETRY OF THE BODY PRESSES FOR THE FINE PUNCHING USING FEM ANALZSIS

Received: 25 August 2014 / Accepted: 25 September 2014

Abstract: *During the design process of vital structural components it is necessary to consider all engineering design aspects including the initial geometry, material selection, nominal loads, global and detailed stress-strain calculations. The objective of the present article is to outline the process of such multiparametric geometry optimization of a press for fine sheet-metal punching by using FEM analysis. An iterative process of the geometry optimization is illustrated on an example of the press exposed to high static loads under strict allowable deflection requirements. The initial press geometry is modified based on the obtained FEM simulation results. The static calculations are then performed repeatedly on the modified press models until the obtained stress and deflection values fell within the permissible limits. The press model adopted in the described process of iterative geometry modifications represents an input for the calculations under dynamic loads.y*
Key words: *optimization of geometry, press, stress, deflection*

Optimizacija geometrije tela prese za fino prosecanje primenom FEM analize. *Pri projektovanju vitalnih strukturalnih komponenti neophodno je razmatrati sve aspekte konstrukcije uključujući početno geometrijsko definisanje, izbor materijala, nominalna opterećenja, globalni i detaljni proračun naponsko-deformacionih stanja. U radu je ilustrovan iterativni proces optimizacije geometrije prese za fino prosecanje lima primenom FEM analize. Prikazan je postupak optimizacije na primeru prese izložene velikim statičkim opterćenjima u uslovima strogih zahteva u pogledu dozvoljenih vrednosti ugiba strukturnih komponenti. Nakon obavljenih proračuna na inicijalnom modelu prese izvršena je modifikacija njene geometrije. Potom su proračuni ponavljani na modifikovanim modelima prese sve dok nisu dobijene vrednosti napona i ugiba u dozvoljenim granicama. Na taj način usvojena, poboljašana geometrija tela prese predstavlja ulazni model za strukturni proračun pod dejstvom dinamičkog opterećenja.*
Ključne reči: *optimizacija geometrije, presa, naponi, ugibi*

1. INTRODUCTION

It has been estimated that 80% of the product price is already determined in the early phase of engineering design, which prompts companies to focus on finding ways to make quick design decisions regarding crucial issues of costs, quality and market demand. This is precisely the main goal of engineering design (hereinafter referred to as »design« for brevity): to develop and manufacture products that are optimized in terms of reliability and quality in the shortest possible time and with minimum cost [1]. In order to achieve this goal the ideal design process must function, as much as possible, in the virtual product development environment. The virtual product models are flexible and allow any number of iterations necessary to reach the optimal solution. The defined virtual model facilitates better visualization and understanding, which results in improvements of both product quality and development efficiency and consequently provides an optimal design solution without any need for avoidable costly and time-consuming redesigns [2].

The virtual product model prepared in a CAD (computer-aided design) package contains all necessary input data that fully describe geometry of all structural components including boundary conditions, as well as information about materials, needed for CAE (computer-aided engineering) analysis. The numerical simulation setup is based on in-depth understanding of the process physics and reliable experimental results used to predict the material flow and determine the distribution of material, stress, temperature, and strain on tools as well as the potential sources of defects and cracks (apptly called the »hot spots« in damage mechanics). The necessary inputs should also take into account properties and microstructure of the product, as well as the assessment of elastic correction and residual stresses. The most widely applied and the most powerful tool for numerical simulation in the CAE is the finite element method (FEM): a discrete analysis technique based on the physical discretization of the computational domain representing the analized structure[3]. In short, the observed continuum with an infinite number of degrees of freedom (DOF) is approximated by a discrete model of interconnected finite elements with finite number of DOF. There are many different types of elements, depending on their shape, linearity and order.

The selection of element types is influenced by various diverse factors including, but not limited to, the nature of the physical problem problem, model geometry, required accuracy, availability within the software[4].

2. SIMULATION TECHNIQUE

The body of the press for fine sheet metal punching (the press body, hereinafter) is the basic module of the sheet metal working unit. Fig. 1 shows a layout of the press body with hydraulic power unit and static and movable parts, which constitute the initial model. Given the complexity of the punch tool geometry and the high tool production price, this type of metalworking is used in large-scale production of parts made of sheet metal.

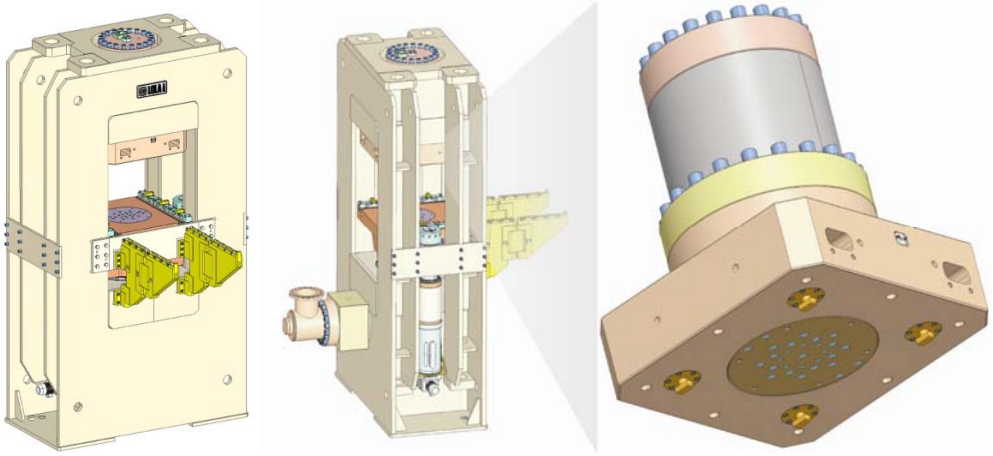

Fig. 1. Three-dimensional (3D) model of the press body

2.1 Initial conditions and constraints of FEM analysis

The computational model of the press body is developed based on the following inputs and assumptions:

- Technical drawing of the initial (draft) version of the press body;
- Mechanical properties of the selected press component materials;
- Load case simulating a static (time invariant) pressure on the appropriate areas of the top and bottom press plates;
- Structure discretization performed by using the 3D quadratic finite elements (number varies between 80 000 and 100 000 elements.)
- Boundary conditions that simulate the press base as rigidly connected to a concrete block that "floats" on an air bag.

2.2 FEM analysis

The main objective of the computation is to determine the deformation and stress fields of the press body resulting from the gravity load and the set of static forces proposed and evaluated by designers. This set of static force values mimics the load transferred from the tool to the press support structure in the course of the press operation [5].

The initial design of the support structure press (called hereinafter the **initial model**) is the first numerical model discretisized by finite elements and supplied with the boundary conditions to simulate the operating conditions. Based on the simulation results obtained by using this model, a series of geometry modifications are gradually introduced accompanied necessarily by their respective FEA calculations. This iterative analytical effort (over ten simulations) resulted eventually in the improved geometry of the press support structure called the **improved model** throughout this article.

The obtained version of the press body model characterized by the static stability is necessary to analyze under the real working conditions—that is, the dynamical loading—before the recommendation for the optimal version of the press body structure is given. The corresponding FEA computation is performed by using the I-DEAS Master Series 12NX software package[6].

1.3 Initial and improved models of the press body and their discretization

As explained before, the initial press body model (Fig. 2a) is used as the starting point for a series of FEM simulations and resulting sequance of successive geometry modifications. This iterative process of gradual geometrical improvements leads finally to the improved model characterized by a strengthened structure of the decreased overall height (Fig. 2b). The strengthening of the improved model is achieved by increase of the widths of the supporting frame and of the horizontal plate placed on the top of the press body[7].

The model coordinate system is positioned in such a way that the *x*-axis is horizontal and oriented to the right, the *y*-axis is vertical and oriented upwards, and the *z*-axis is oriented toward the observer (Fig. 2a).
Fig. 2b illustrates the 3D geometry model of the existing improved version of the press body. The structural analysis culminated in the upgraded version of the improved press body model preloaded with four M140 bolts (150 mm in diameter) and the preloading force of 1500 kN per bolt (Fig. 2b).

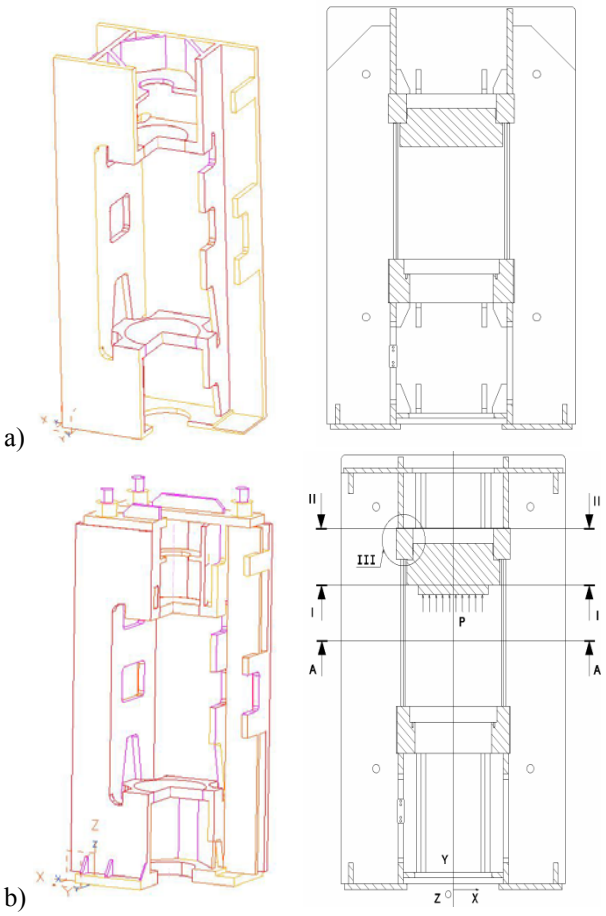

Fig. 2. The press body: a) initial model, b) improved model

The deformation and stress fields of the press body are obtained for the boundary conditions which simulate the its footing rigidly fixed to the concrete block "floating" on an air bag. Note that the influence of the concrete block and the air bag is disregarded. In other words, the problem of boundary conditions is solved by disabling displacement on the bottom surface of the press body footing in all directions [8,9].

The static FEA simulation is performed for the worst-case load scenario by simulating the pressure on the appropriate surfaces of the top clamping plate and the bottom plate of the press body. The simulation is performed for the static force of 6300 kN resulting from the punching tool, that is, it from the movement of the top and bottom movable parts of the press body [10].

The centered load is applied on both the initial and the improved model, while the eccentric load on the later only. These load cases represent the static-force variants of the load encountered under regular operating conditions, and encompass two extreme cases of eccentric load that can occur during operation [11,12]. The load consists of the weight of the press body itself and the static force, which has three variants:

- centered load: F=6300 kN (Figure 3a),
- eccentric load shifted along the x-axis by 235 mm: where the force F_1=4800 kN is centered, and the force F_2=1500 kN is exerted eccentrically (Fig. 3b),
- eccentric load shifted along the z-axis by 150 mm; where the force F_1=4800 kN is exerted centrally, and the force F_2=1500 kN is exerted eccentrically (Fig. 3c).

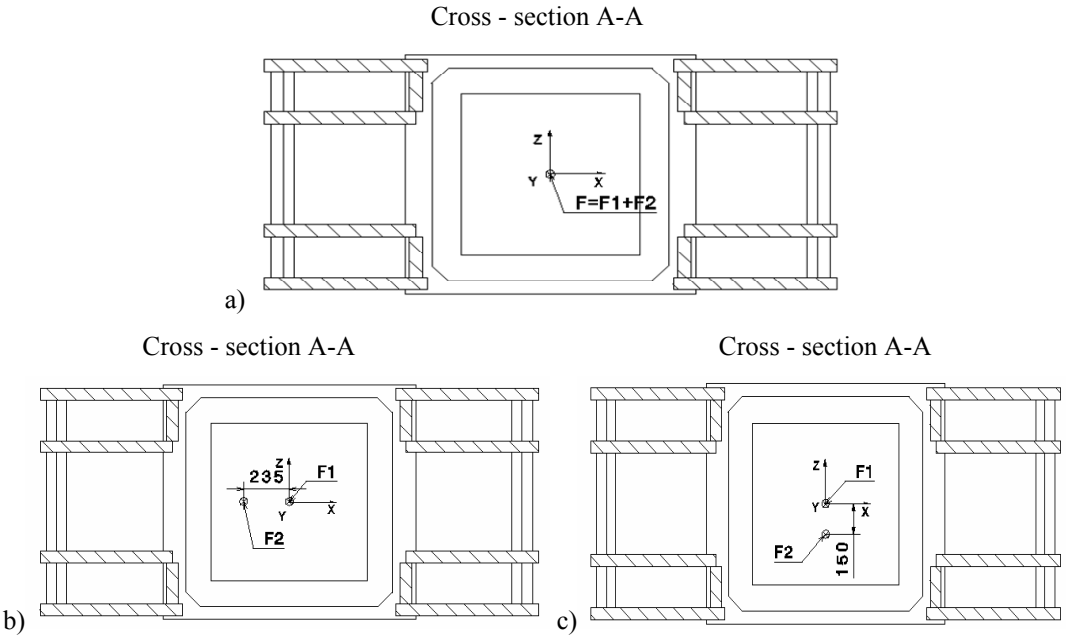

Fig. 3. Loads: a) Centered, b) Eccentric shifted along the x-axis and c) Eccentric shifted along the z-axis

3. RESULTS AND DISCUSSION

3.1. Simulation results for the initial model

The deformation field of the entire press body is presented in Fig. 4a. The maximum value of deformation (depicted by red color) is 1.56 mm on the upper plate. The lower part of the model exposed to the

static load behaves in stable manner with less pronounced deformation (up to 0.863 mm – the yellow-green areas). The top part of the structure exhibits a much more significant distortion by opening toward the top. The ends of the outer plates bend outwards, while the two transversal ribs bend considerably along the *z*-axis. When the overall deformation is decomposed into displacements along three coordinate axes, it can be observed again that the displacement along the *y*-axis is small for the bottom plate of the press body (−0.144 mm), but considerable on the top plate (0.328 mm). This deformation is along the load direction and is therefore expected. However, a considerable displacement along the *x* and *z*-axis is also noticeable (in excess of 0.320 mm at the top part of the structure).

Von Mises equivalent stress has a uniform distribution in the press body, with a value up to 80 N mm^{-2} (Fig. 4b). The maximum stress value (500 N mm^{-2}) appears locally at the points of connection of the upper/bottom plates with the press body (vertical walls). σ_{xx} and σ_{zz} values are 80 N mm^{-2} in contrast to σ_{yy} which reaches 156 N mm^{-2}.

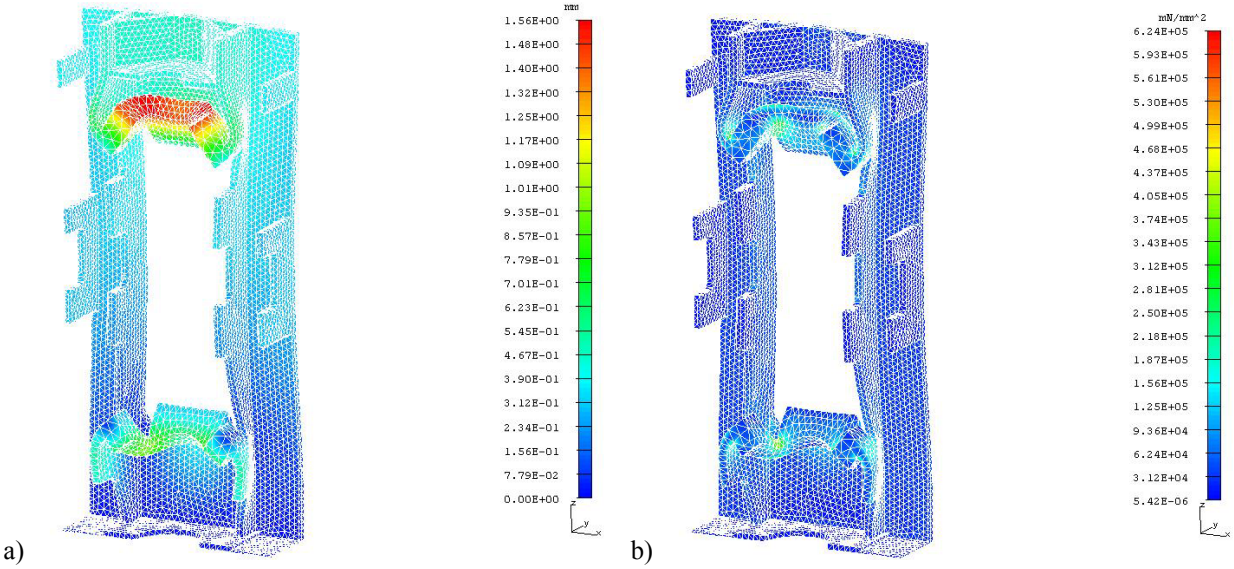

a) b)

Fig. 4. Initial model: a) deformation field, b) von Mises stress field

3.2. Simulation resulats for the improved model

An FEA computation is performed on the press working plate as a separate part to verifying the computation results of the press body. Fig. 5 illustrates a 3D geometry model of the working plate, which is statically loaded with the same force used previously to mimics the the operational load of the press (6300kN). The boundary limitations are defined at the connection points of the working plate and of the body presses.

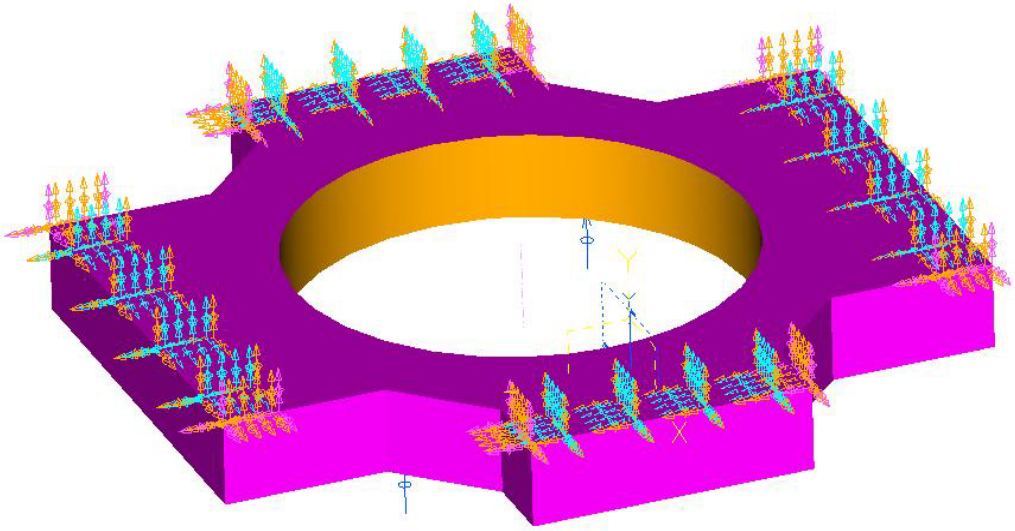

Fig. 5. 3D geometry model of the press body working plate

The maximum deformation of the working plate (depicted with red color in Fig. 6a) is 0.5 mm. This deformation of the working plate affects the total press-body deformation by superposing it with the deformation of the press body wall at their mutual connection points. Von Mises stress distribution (Fig. 6b) in the working plate is of the same maximum value and spatial distribution as in the case when the working plate is an integral part of the initial press model.

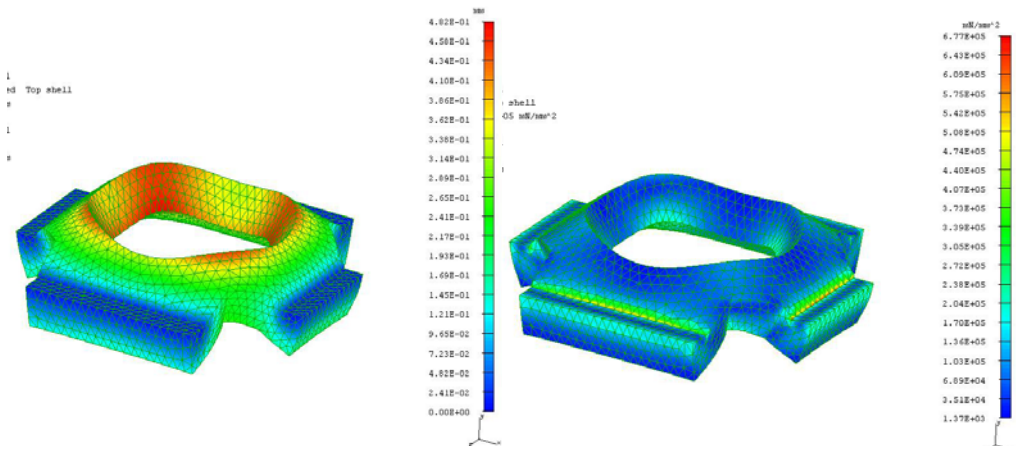

Fig. 6. Press working plate: a) deformation fiels, b) von Mises stress field

Fig. 6a shows that the structural deformation at the connction points of the press wall and the upper working plate is 0.8 mm. Therefore, the press wall deformation superposed on the deformation of the working plate results in total deformation of 1.5 mm of the initial model at the point of the upper working plate.

The accuracy of the analysis is confirmed by the deformation value computed for the plane corresponding to the upper surface of the lower working plate as shown in Fig. 6b. The structure deformation is 0.3 mm at the connection points of the press wall and the lower working plate. By superposing this deformation on that of the working plate as a separate part a total deformation of 0.8 mm of the initial model at the point of lower working plate is obtained.

The von Mises stress distribution at the lower surface of the upper working plate (Fig. 8.) reveals a stress increase at the point of connection of the working plate and the press wall.

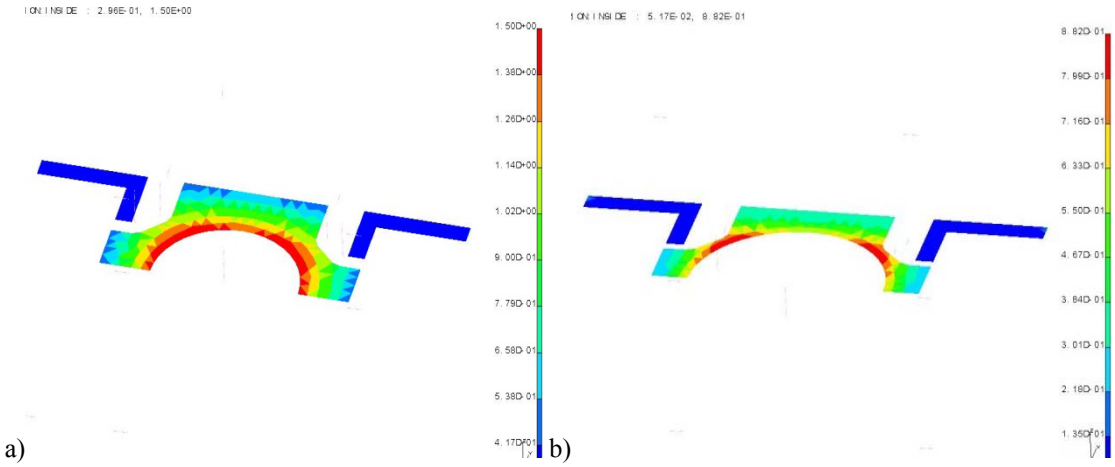

a) b)

Fig. 7. Deformation distribution in the plane corresponds to: a) the lower surface of the upper working plate, b) the upper surface of the lower working plate

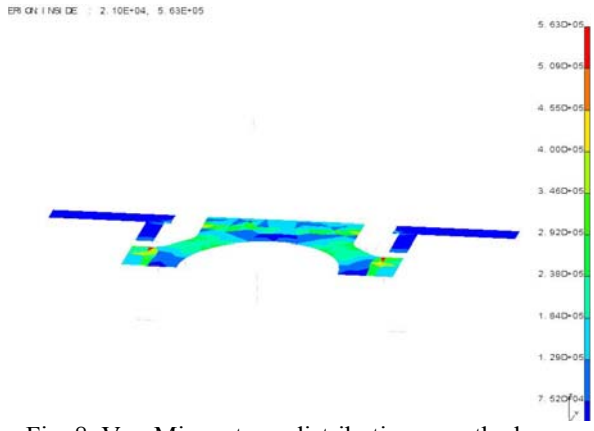

Fig. 8. Von Mises stress distribution over the lower surface of the upper working plate

3.3. Deformation and stress of the improved press model

The deformation distribution of the improved press model (Fig. 9a) reaches a maximum value of 0.51 mm on the upper plate. The Fig. 9a illustrates a steadier behavior of the whole model of the press body compared to the corresponding deformation of the initial model (1.5 mm). The von Mises stress distribution in the upgraded model (Fig. 9b) is uniform and the value is up to 30 N mm^{-2}. The stress increase at the point of connection of the lower plate to the press body reaches 260 N mm^{-2}.

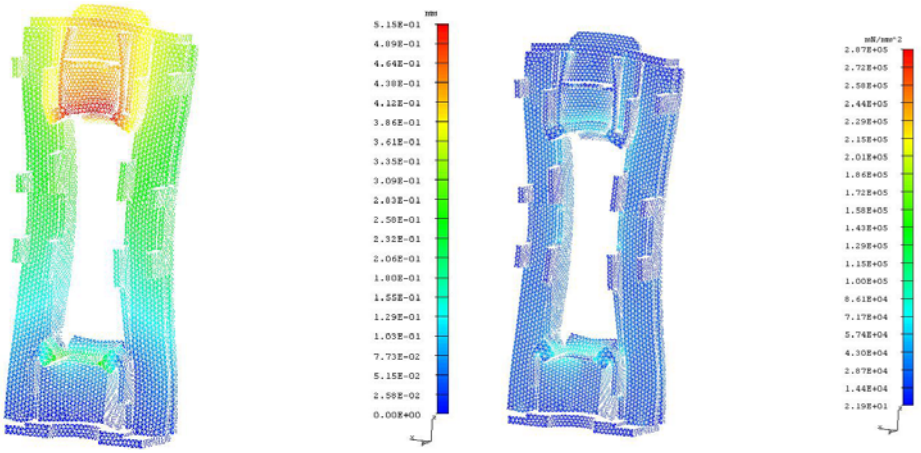

Fig. 9. Upgraded model: a) deformation distribution, b) von Mises stress distribution

The press body models defined so far do not capture realisticaly the actual stress and deformation fields since the press body is given without clamping plates for tools and other structural elements that affect rigidity of the press. When the clamping plates and additional bracings are oncluded into the FEA model, a completely different stress and deformation distributions are obtaines as illustrated henceforth.

3.4. Deformation and stress for the improved press model with additional bolts for preloading

The maximum deformation of the upgraded press body model with additional bolts for preloading (Fig. 10a) reaches 0.27 mm at the lower clamping plate. This implies that the use of bolts for preloading reduces the deformation of the press wall, which leads to a lower total value of deformation.

Von Mises stress distribution in the upgraded model with additional preloading bolts (Fig. 10b) is relatively uniform with a very low value of up to 30 N mm^{-2}. A localized stress increase, limited to just a few finite elements, at the point of recline of the upper plate on the upper press body reaches 180 N mm^{-2}.

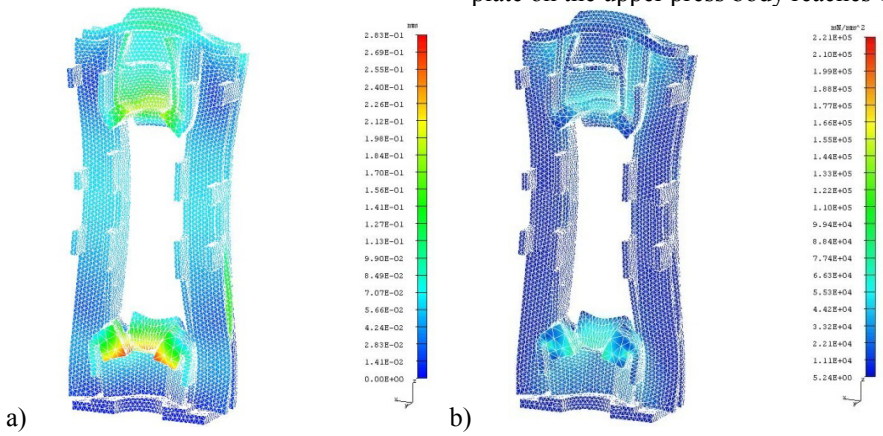

a) b)

Fig. 10. The upgraded model with additional preloading bolts: a) deformation distribution and b) von Mises stress distribution

Fig. 10 shows that the deformations in the x and z directions are 0.116 mm and 0.109 mm, respectively, while it reaches 0.306 mm along the y-axis. This means that the improved model deformations in the x and z directions decreased threefold in comparison with the respective initial model displacements.

Von Mises stress distribution in the improved model (Fig.10b) is uniform with relatively low maximum value, 33.5 N mm^{-2}. A stress increase appears at the point of recline of the top clamping plate on the top plate and reaches 168 N mm^{-2}. σ_{xx} and σ_{zz} maximum values are below 95 N mm^{-2}, while in σ_{yy} maximum value reaches 177 N mm^{-2}.

3.5. Characteristic values of displacement and stress

Fig. 11 illustrates the points on the top plate and on the top clamping plate of the press body at which the values of deflection and stress are evaluated. The cross-section I-I shows the disposition of evaluation points on the top clamping plate (the horizontal surface on the bottom side), from point 1 to point 4 (Fig. 11a). The cross-section II-II shows the disposition of evaluation points on the top plate of the press body (the horizontal plate on the top side), from point 1 to point 4 (Fig.11b).

Planarity of the loaded surfaces of the clamping plate is 0.025 mm, 0.110 mm, and 0.100 mm in the cases of the centered load, the eccentric load along the x-axis, and the eccentric load along the z-axis, respectively.

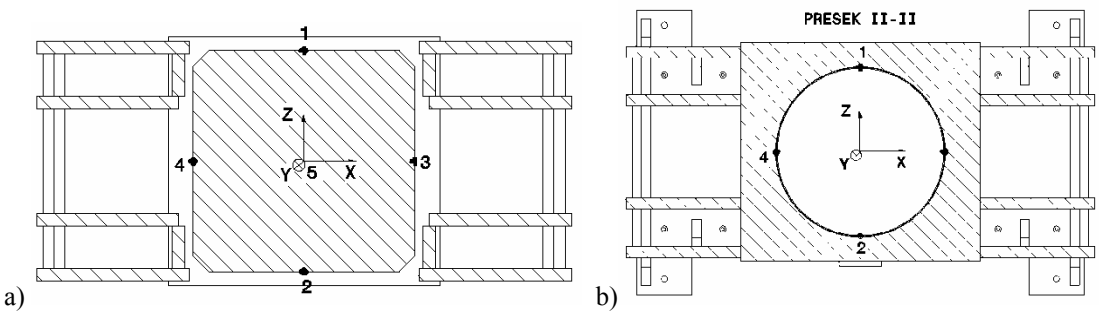

a) b)

Cross - section I-I Cross - section II-II

Fig. 11. The evaluation points disposition on: a) the top clamping plate and b) the top plate.

4. CONCLUSION

The static FEA simulations performed in the present article enable an insight into the deformation and stress distributions of the initial press model and emphasized the need for necessary changes in geometry. These structural modifications that have been made in the initial model resulted in the improved model, which have proved to be statically more stable. These geometry modifications also proved to be beneficial from the standpoint of the press overall mass which decreased 450 kg.

In order to interpret properly the stress and deformation values in the postprocessing phase of the FEM analysis, it is necessary to focus on certain press parts. The simulation results indicate that the maximum stress values in the two models are not significantly different (81 N mm^{-2} and 90.3 N mm^{-2}). It is important emphasized, thought, that these stress values, for both the centered and the eccentric loads, are well below the distortion limit of the selected steel, which is 248 N mm^{-2}. Although the simulation results on the upgraded model with additional clamping plates indicate, the stress criterion (σ=0.5 σ_{02}) is not satisfied for the corresponding sheet metal Č.0361. The deformation criteria for the press body are satisfied.

Finally, it cannot be overstated that in order to accept the improved model conceptual design, it is necessary perform an adequate dynamic FEA simulation with realistic loads and perform an analysis of obtained solutions.

5. ACKNOWLWDGEMENTS

The results presented in this paper originated partially from Research Project TR funded by the Ministry of Education and Science of the Republic of Serbia.

6. REFERENCES

[1] Jedrzejewski, J., Kwasny, W. (2001). XII *Workshop, on Supervising and Diagnostic of Machining Systems*, Wroclaw University of Technology.

[2] Mandic V. (2012). *Physical and numerical modeling of metal forming processes.* Faculty of Engineering, University of Kragujevac, Kragujevac, Serbia.

[3] Weck, M., Hessel, C. (2002), *Flächenrückführung topologieoptimierter FE-Modelle*, WT Werkstattstechnik online 92 H. 7/8, Springer-VDI-Verlag, Düsseldorf, pp. 377-381.

[4] Kojic M., Slavkovic R., Živkovic M., Grujovic N. (2010). *Finite element method*. Faculty of Engineering, University of Kragujevac, Kragujevac, Serbia.

[5] Cook, R., Malkus, D., Plesha, M. (1988). *Concepts and Applications of Finite Element Analysis*, 3 Edition, John Wiley, Madison.

[6] Altintas Y., Brecher., Weck M., Witt S. (2005). Virtual machine tool, *CIRP Annals - Manufacturing Technology*, Volume 54, Issue 2, pp. 115–138.

[7] Bern M., Plassmann P. (2000). *Mesh generation*. Handbook of computational geometry, Elsevier Science, Amsterdam, pp. 291–332.

[8] Herz E., Hertel O., Vormwald M. (2011). Numerical simulation of plasticity induced fatigue crack opening and closure for autofrettaged intersecting holes. *Engineering Fracture Mechanics*, vol. 78, pp. 559–572.

[9] Döring R., Hoffmeyer J., Seeger T., Vormwald M. (2003). A plasticity model for calculating stress–strain sequences under multiaxial nonproportional cyclic loading. *Computational Materials Science,* vol. 28, no. 3–4 pp. 587–596.

[10] Dowling N., (2003). *Local strain approach to fatigue, comprehensive structural integrity*. Elsevier, vol 4, pp. 77–94.

[11] Sauve R.G., Morandin G.D. (2004). Simulation of contact in finite deformation problems–algorithm and modeling issues. *International Journal of Mechanics and Materials in Design*, vol. 1, pp. 287–316.

[12] Belytschko T. (1986). Hughes T.J.R., (eds.) *Computational Methods in Mechanics*, Vol. 1. North-Holland Elsevier Science.

Authors: **M.Sc. Radomir Radisa, Dr. Srecko Manasijevic, M.Sc. Velimir Komadinic,** Lola Institute, Belgrade, Serbia, www.li.rs, **Prof. Dr. Vesna Mandic, Prof. Dr. Milentije Stefanovic,** Faculty of Engineering, University of Kragujevac, Kragujevac, Serbia, www.mfkg.rs.
E-mail: radomir.radisa@li.rs,
srecko.manasijevic@li.rs